Eur. Phys. J. D **6**, 487–493 (1999)

**THE EUROPEAN PHYSICAL JOURNAL D**

EDP Sciences


# Measurement of the Majorana effect in a molecule using a switched magnetic field and quantum beat detection

H. Ring, R.T. Carter, and J.R. Huber[a]

Physikalisch-Chemisches Institut der Universität Zürich, Winterthurerstr. 190, 8057 Zürich, Switzerland

Received: 4 February 1999

**Abstract.** By means of quantum beat spectroscopy we investigated the dynamics of magnetic moments associated with hyperfine levels in the molecule $^{13}CS_2$ under "spin-flip conditions". Oriented molecules in a cold beam were prepared by excitation with a circularly polarized laser pulse ($\tau \sim 3$ ns) in a weak magnetic field ($B = 5.4$ G). Subsequently, they were exposed to a rapid field inversion which left the magnetic moment in its initial orientation. The initially created coherences among the excited hf levels were conserved after field reversal and thus were explored to characterize the changes in the level structure due to this "Majorana spin-flip" process.

**PACS.** 42.50.Md Optical transient phenomena: quantum beats, photon echo, free-induction decay, dephasings and revivals, optical nutation, and self-induced transparency – 33.55.Be Zeeman and Stark effects – 32.80.Qk Coherent control of atomic interactions with photons

## 1 Introduction

Coherent time domain spectroscopy in the optical regime, commonly referred to as quantum beat spectroscopy, is a powerful tool owing to its essentially Doppler-free nature and a high-resolution power which is limited only by the lifetime of the coherently excited states [1,2]. For studies such as the dynamics and the spectroscopy of Zeeman levels and of the hyperfine structure in electronically excited molecules the method has proven to be extremely useful as demonstrated for a number of molecules [3–5] under beam conditions. Recently, this method has been extended by replacing the stationary magnetic or electric field with a time-dependent external perturbation of the molecule. Thus by means of an optical-RF–double resonance experiment the transfer of population and coherences was monitored by quantum beat measurements [6,7] and very recently the latter method allowed us to demonstrate the creation and manipulation of coherences in a molecule using switched magnetic fields [8,9].

In the present work we employed detection of coherences by quantum beat spectroscopy to study the spin dynamics in a molecule under the influence of a rapidly changing magnetic field. Effects due to such a perturbation are known as "Spin Flip Transitions" or "Majorana transitions"[10–14]. They occur in an atomic or molecular beam with a given spin polarization when travelling in a magnetic field with locally varying strength and orientation. The passage of the atomic or molecular species near a point where the magnetic field is reversed will induce a change in the orientation of the spins with respect to the local magnetic field. Such nonadiabatic processes were shown to take place if the Larmor precession frequency is slow compared to the rate of change of the direction of the magnetic field in the proximity of the zero-field point. The problem of a spin in a varying magnetic field has been extensively studied [10–18]. Newer applications have gained interest which are concerned with the preparation or selection of spin states [19,20] and transfer of population among spin states [21], not least because of possible applications in quantum computing [22,23].

Unlike the previous studies on the Majorana effect which employed a continuous atomic beam, we carried out a pulsed molecular beam experiment in combination with a switched magnetic field where the latter is homogeneous over the probe volume. As a model system we used the $^{13}C$ isotopomer of the $CS_2$ molecule which possesses a nuclear spin $I = \frac{1}{2}$. This triatomic molecule has been studied quite extensively in the past, so that the convenient electronic transitions in the 30000 $cm^{-1}$ excitation region are well characterized also for the $^{13}C$ isotopomer [24–27]. The excited electronic states have fluorescence lifetimes on the order of microseconds allowing us with Fourier transform limited nanosecond laser pulses to coherently excite Zeeman and hyperfine levels [26,27] with a high selectivity and to monitor their decays in the presence of a fast switched magnetic field.

## 2 Experimental details

A detailed description of the laser system may be found elsewhere [4,6]. Briefly, the output of a pulsed dye

[a] e-mail: jrhuber@pci.unizh.ch

amplifier, seeded by a single mode ring laser (Coherent 699-29), was frequency doubled yielding horizontally polarized laser pulses with a Fourier transform limited bandwidth ($\Delta\nu \sim 180$ MHz, $\Delta t \sim 3$ ns) and an energy of 50-100 $\mu$J/pulse. Linear polarization in an arbitrary direction was obtained by sending the light through a polarization rotator composed of two Fresnel rhombs and subsequently through a Glan-Taylor polarizer. Circularly polarized light was produced by passage of the frequency doubled laser beam through a polarizer for elimination of spurious amounts of circular polarization and then through a single Fresnel rhomb rotated at $\pm 45°$ for obtaining left/right-handed light. Tilting of the Fresnel rhomb was achieved by a precision rotator as the the quality of the circular polarization (*i.e.* the deviation from a perfectly circular polarization towards a slightly elliptical one) depended critically on the tilt angle. With a given polarization, the laser pulses entered into the vacuum chamber where they intersected a pulsed supersonic molecular jet about 40 mm downstream from the nozzle. In the pulsed jet, isolated and very cold ($T_{\rm rot} \sim 4$ K) molecules were produced by expanding a mixture of 2.5% $^{13}CS_2$ in 1 bar neon through a 0.3 mm aperture mounted on a pulsed piezoelectric valve. We used a 99% enriched sample (Cambridge Isotope Laboratories) outgassed prior to use, whereas preliminary measurements were taken with the 1% natural abundance of $^{13}CS_2$ in normal samples. Fluorescence from the center of the molecular beam was selected by focusing through a 1 mm slit aperture and detected by a photomultiplier tube (PMT, Hamamatsu R329-02). Placing sheet polarizers before the PMT allowed selection of a linear polarization of the detected fluorescence. The resulting signal was fed to a digitizing oscilloscope (Le Croy 9450) and stored on computer as a series of 2048 data points with a time step of 10 ns. Initial trigger pulses for the pulsed valve and laser were provided by the computer. As a more precise timing between the acquisition of the decay and the magnetic field pulses was required, the oscilloscope and pulsed field circuit (see below) were triggered by the laser pulse which was detected by a second photomultiplier tube on a secondary reflection. This procedure reduced the time-jitter in the recorded emission decays (typically 4000 shots) to $< 5$ ns.

In total five sets of Helmholtz coils were used for the generation of the desired magnetic field. The Earth's magnetic field was compensated by three sets of large coils placed around the vacuum chamber. One additional pair of coils generated a constant magnetic field of 5.4 G the direction of which was antiparallel to the laser propagation direction. In contrast to previous works [6,8], we define a coordinate system such that the laser beam was directed along $-Z$, and the constant field along $+Z$. This field could be reversed with an arbitrary delay after a laser shot by switching on an opposite field (directed along $-Z$) of twice the strength (10.8 G). The equality of the moduli of the magnetic fields before ($B_Z$) and after ($-B_Z$) switching was verified experimentally (*vide infra*). The magnetic field pulses were provided by a pair of small Helmholtz coils with diameter 55 mm and 7 windings per coil which were placed around the crossing of laser and molecular beams. A more detailed description of the home-built switching circuit can be found elsewhere [9]. The risetime of the switched field was about 100 ns, and it was switched off only after the recording of the fluorescence decay.

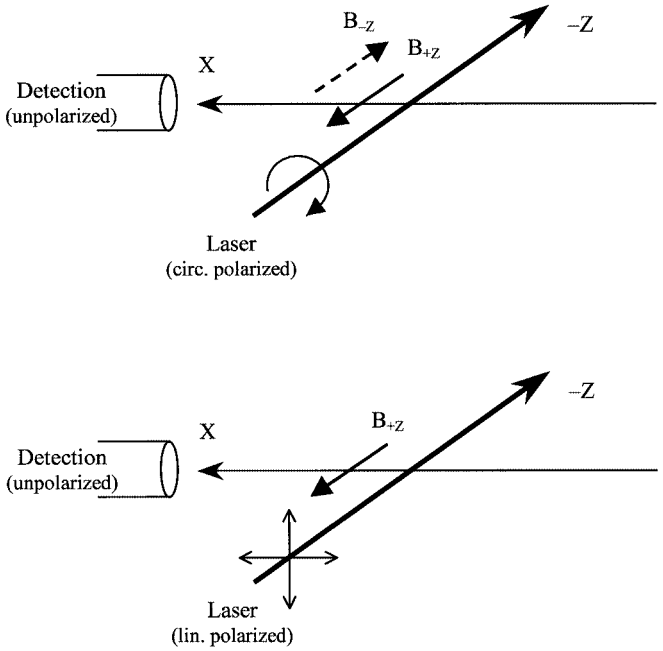


**Fig. 1.** Geometrical arrangement for excitation and magnetic field orientation. The upper part refers to excitation with circularly polarized light and reversal of the magnetic field, while the lower part shows the situation when excitation with linearly polarized light is used. As the magnetic field is perpendicular to the polarization vector in the latter case, $\Delta M'_F = 0, \pm 2$ coherences are observed.

## 3 Results

The geometrical arrangement used in this work is depicted in Figure 1. Excitation with linearly polarized laser light was chosen (lower part) for preliminary experiments to demonstrate the accessible coherences among the excited hyperfine levels for collinear laser and magnetic field directions, while the actual spin-flip experiment was carried out with circularly polarized laser pulses (upper part). In both cases, excitation took place in a magnetic field $B_Z$ which was antiparallel to the direction of the incoming laser pulse (along $-Z$). For the spin-flip experiment, the magnetic field was reversed after a variable delay relative to the laser pulse, whereas it was maintained constant for the preliminary measurements. Fluorescence emission of the molecules was detected at right angles to the laser axis (along $X$) and without selection of a particular polarization.

The $^{13}CS_2$ molecule with nuclear spin $I = \frac{1}{2}$ has a total angular momentum $\mathbf{F} = \mathbf{J} + \mathbf{I}$, where $\mathbf{J}$ is the rotational angular momentum of the molecule. Although the

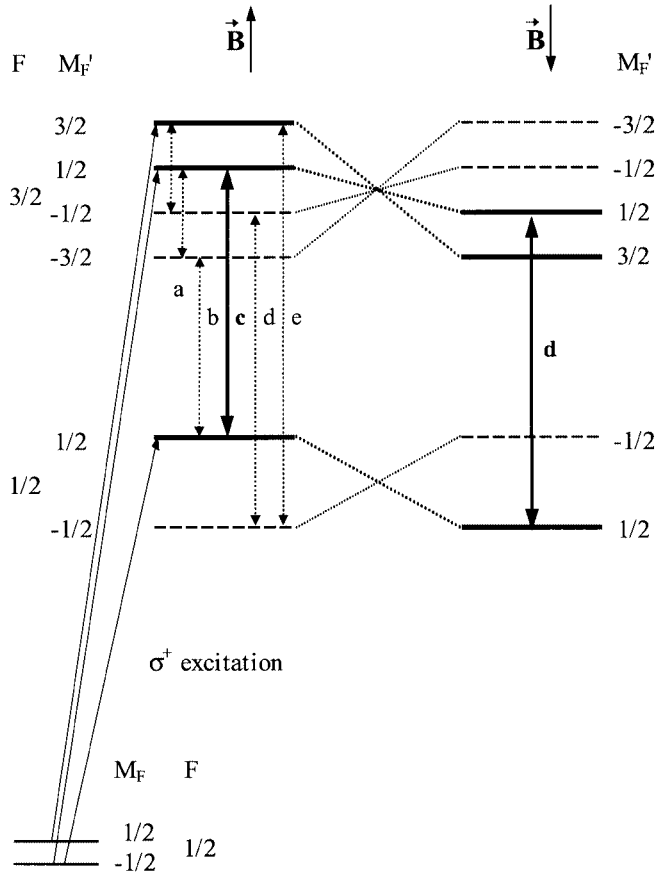


**Fig. 2.** Scheme of the participating levels. The letters (a) to (e) are used to indicate the coherences between particular levels. The corresponding quantum beats are displayed in Figure 3. For the assignment of the molecular eigenstates we used a space fixed coordinate system. In this representation the same states are populated before and after reversal of the magnetic field.

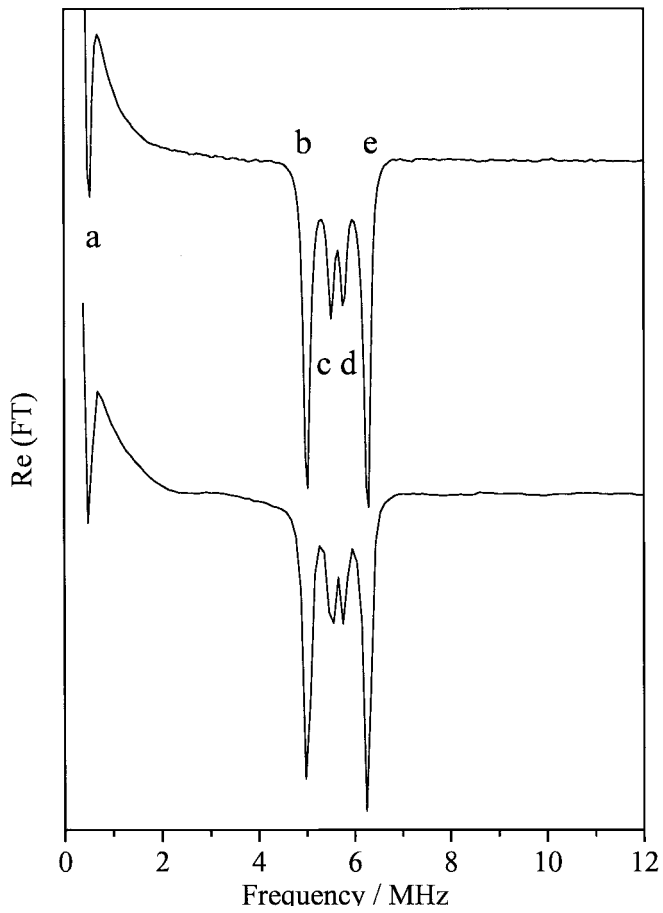


**Fig. 3.** Fourier transforms of the decays following excitation with linearly polarized light. The lower trace corresponds to a decay process where the constant magnetic field was applied in the $+Z$-direction. In the upper trace, the switched field with double magnitude in the $-Z$-direction was also present and was triggered before the laser pulse. The result demonstrates the equality of the moduli of the effective fields before and after switching, and also the identical shape of the Fourier transform in both field directions. The letters (a) to (e) refer to the coherences indicated in Figure 2.

excited electronic state $V^1B_2$ is a singlet state, its rotational eigenstates possess an electron spin magnetic moment **S** due to the spin-orbit coupling with triplet states [27,28] in which a spin uncoupling interaction is active [26]. Interaction of the magnetic moments of the electron and nuclear spins **S** and **I** gives rise to a splitting $\Delta E_{\rm hf}$ between the hyperfine (hf) states $F' = J' \pm \frac{1}{2}$. As the $^{32}$S atoms are bosons, only rotational levels with odd $J'$ exist in a $K' = 0$ stack in the excited electronic state, making $J' = 1$ the lowest possible excited rotational level. Experiments were performed by exciting an $R(0)$ transition of $^{13}C^{32}S_2$ at 30873.72 cm$^{-1}$ which starts from the electronic ground state $\tilde{X}\ ^1\Sigma_g^+$ to the $V^1B_2$ electronic state via the 10 V band [24,25]. The $J' = 1$ upper level has hf states $F' = \frac{3}{2}$ and $F' = \frac{1}{2}$ with a hyperfine splitting $\Delta E_{\rm hf} = 5.63$ MHz and a radiative lifetime of 2.1 $\mu$s [27]. Application of an external magnetic field removes the $(2F' + 1)$-fold degeneracy yielding the four sublevels $M_F' = \pm\frac{3}{2}, \pm\frac{1}{2}$ for $F' = \frac{3}{2}$ and the two sublevels $M_F' = \pm\frac{1}{2}$ for $F' = \frac{1}{2}$ as shown in Figure 2. Therefore it is noted that we did not observe the dynamics of a sole spin in a magnetic field, but of an angular momentum $F'$ possessing a magnetic moment. In our experiments, we remained in the weak field (Zeeman) limit where both $F'$ and $M_F'$ are good quantum numbers. As the electronic ground state does not possess a magnetic moment, the two components $F'' = I = \frac{1}{2}, M_F'' = \pm\frac{1}{2}$ of the starting level $J'' = 0$ of the excitation transition remain effectively degenerate in the presence of a magnetic field. For the sake of clarity however, they are plotted with a finite splitting in Figure 2 where the left-hand side also reproduces schematically the ordering of the excited state sublevels.

Upon coherent excitation of this set of sublevels by a short laser pulse, different coherences are created depending on the geometry of the experiment, where "geometry" refers to direction and polarization of excitation and detection, and the orientation of the magnetic field. A linearly polarized laser pulse generates six coherences among the six sublevels using the geometry given in Figure 1. In this

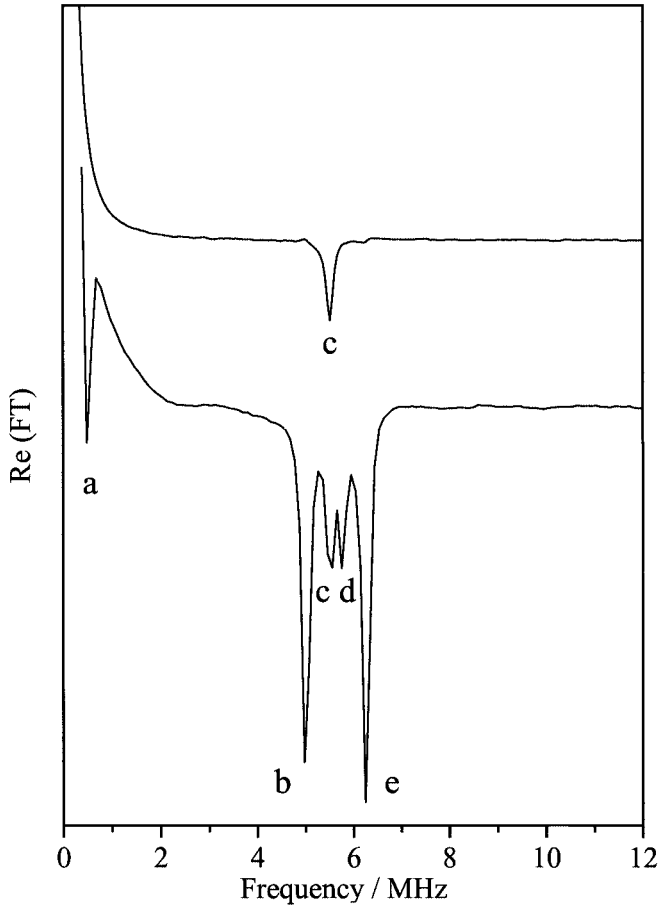


**Fig. 4.** Fourier transforms of decays obtained without field reversal after linearly (lower trace, from Fig. 3) and circularly (upper trace) polarized excitation. Here, the magnitude of the zero frequency peaks in the Fourier transforms are normalized so that the strengths of the different coherences can be compared.

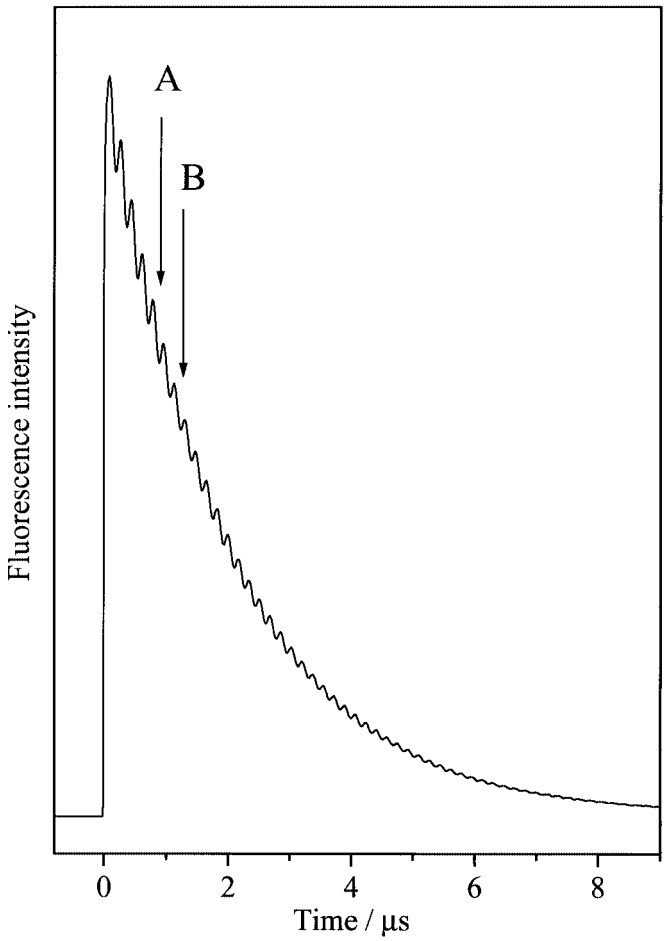


**Fig. 5.** Example of a fluorescence decay signal. Excitation has taken place via a $R(0)$ line in the 10 V vibrational band ($V^1B_2$ electronic state) of $^{13}CS_2$ at 30873.72 cm$^{-1}$. The first arrow (A) designates the onset of the switched magnetic field 0.85 $\mu$s after the laser pulse while the second (B) at 1.28 $\mu$s after excitation indicates the starting point for the Fourier transform given in Figure 6 (solid line).

arrangement, the laser polarization is necessarily perpendicular to the magnetic field and thus defines the selection rule $\Delta M'_F = 0, \pm 2$ for the coherences; we obtain five beat frequencies as expected for hf polarization quantum beats [4,5,26]. The result of the measurement is shown in Figure 3, where the upper trace corresponds to the Fourier transform of the decay recorded after excitation in a static magnetic field oriented antiparallel to the direction of light propagation, whereas for the lower trace, the direction of the static magnetic field was reversed before the excitation process. Both orientations yield obviously the same decay and the same beat pattern, assuring us that no artifacts are involved and that the magnitude of the magnetic field was the same before and after field reversal. The labels (a)-(e) which we used to identify the different beat frequencies (similar to Figure 6 in reference [26]) in Figure 3 refer to the coherences among the hyperfine levels shown in Figure 2 (left side). For the beat frequencies (a) to (e) in a field of 5.4 G, we find the values 0.51, 5.01, 5.52, 5.78 and 6.27 MHz.

The reflection symmetry with regard to a plane perpendicular to the $Z$-axis is lost when excitation with circularly polarized light is applied. The transitions indicated in the level scheme on the left-hand side of Figure 2 correspond to excitation with $\sigma^+$ polarized light, obeying the selection rule $\Delta M_F = +1$. Hence only three among the six hyperfine levels are populated. As the transitions towards the two levels with $M'_F = \frac{1}{2}$ start from a different ground state level than the transition towards the level with $M'_F = \frac{3}{2}$, a coherence is created only between the first two levels, and *a single beat frequency* (c) is observed. The Fourier transform of a decay recorded according to the left-hand side of Figure 2, using a static magnetic field and circular $\sigma^+$ polarization, is given in Figure 4 (upper trace), together with the reproduction of the result for linear polarization, as taken from Figure 3. Comparison of the two traces clearly shows the survival of beat (c) exclusively, thus indicating the preparation of molecules with a polarized (oriented) total angular momentum $F'$. Very

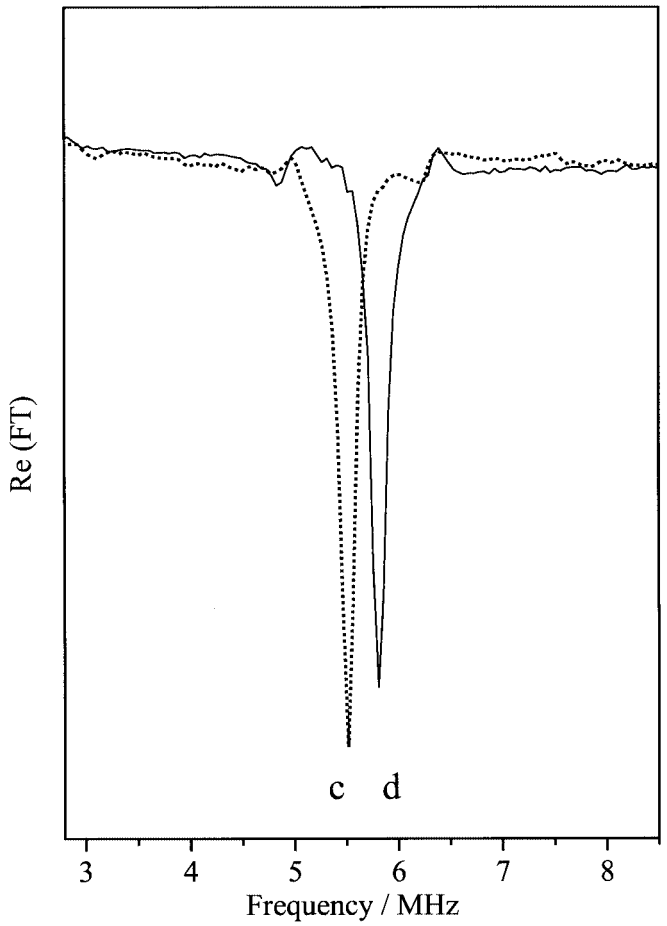


**Fig. 6.** Fourier transforms of decays following excitation with circularly polarized light. In the dotted trace (left peak), excitation and decay take place in a static magnetic field ($+Z$ direction). In the solid trace (right peak), the magnetic field was reversed about 0.85 $\mu$s after the excitation process. The Fourier transform was taken only from the part of the decay in which the field was completely reversed (see Fig. 5). The zero frequency peaks of the two Fourier transforms have been normalized. In both cases, the weak structure at the base of the main peak is due to the beats (b) and (e) and is caused by a slight imperfection in the circular polarization.

weak peaks persist in the Fourier transform at the frequencies (b) and (e) which are due to a slight imperfection of the circular polarization. By comparison of measurements with linear and circular polarization it can be concluded that the linear polarization in the latter measurements was suppressed to less than 3%.

These preliminary measurements in a static magnetic field serve as a basis for the understanding of the central experiment, which aims to observe the effects which occur when the magnetic field is reversed *after* excitation. To this end, circularly polarized excitation was used for the preparation of a polarized superposition state in a constant magnetic field, as described in the previous paragraph. After a given delay, the switched field was turned on. Due to its finite risetime, the complete reversal from $\mathbf{B}$ to the opposite field $-\mathbf{B}$ was attained approximately after 200 ns. After this delay, the magnetic field remained constant, allowing the subsequent emission decay to be analyzed. An example for the timing of such an experiment is given in Figure 5 by means of a recorded emission decay. The first arrow (A) indicates the time of onset of the transient magnetic field, the second (B) defines the starting point for the Fourier transform. The result of the switched field experiment is shown in Figure 6 (full line), together with the Fourier transform stemming from a decay in a constant magnetic field (dotted line). Compared to the latter, the beat observed after fast field reversal is shifted towards higher frequencies. As the modulus of the magnetic field vector $|\mathbf{B}|$ regained its initial value after complete field reversal, this behavior cannot be due to a modification of the beat frequency in a different magnetic field. Actually, the new beating frequency corresponds exactly to the frequency of coherence (d) in Figure 2. This clearly indicates that changes in population and coherences among the hyperfine levels have occurred. Concerning the appearance of the Fourier transform of the switched experiment, two points are noteworthy. First, no significant difference of the linewidth of the peak corresponding to frequency (d) with those of experiments in constant fields can be found. Second, the modulation depth of the beat which is given by the ratio of the beat frequency peak to the zero frequency peak in the Fourier transform is slightly changed. In Figure 6, the two traces have been scaled to give identical zero frequency peaks but peak (d), corresponding to the switched experiment, is slightly lower. This effect was found in all of our field reversal measurements revealing a weak dephasing. Finally, the experiment was repeated for different delays of the switched magnetic field, but no dependence on this parameter was observed within the precision of the measurements.

## 4 Simulation

In previous work on Majorana spin-flips, the effect of magnetic field reversal was generally investigated by analytical methods [10,11,16] which often restricted discussion to limiting cases. Numerical simulations, however, provide a general and convenient tool for comparing experimental results with quantum-mechanical calculations. In order to simulate our experimental results, we applied a density matrix approach [29,30] as detailed in our previous work [8], with the calculation of the excitation and detection matrices being extended to take account of the hyperfine structure and to model both linear and circular polarized light. The excited state density matrix is given by $\varrho_{MM'} = \sum_i F_{MM'}\varrho_{ii}$, where $F_{MM'}$ and $\varrho_{ii}$ are the excitation and (diagonal) ground state matrices, respectively. The time dependence of the excited state density matrix is given by the Liouville equation

$$\frac{\partial \varrho}{\partial t} = \frac{1}{i\hbar}[\mathbf{H}, \varrho]. \tag{1}$$

In the weak field limit, the Hamiltonian for hyperfine levels in a magnetic field is written as $\mathbf{H} = \mathbf{H_0} + g_F\mu_\mathrm{B}\mathbf{B}\cdot\mathbf{F}$,

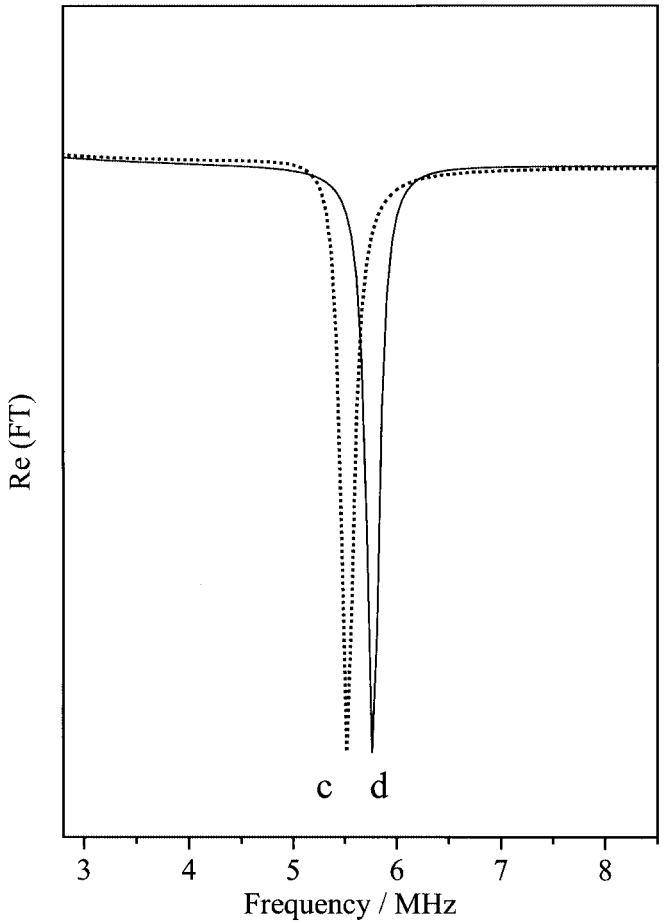


**Fig. 7.** Simulation of the spin-flip experiment. The dotted trace is the Fourier transform of a decay which occurs in a constant magnetic field, the full line corresponds to the case where the field is reversed after excitation. As for Figure 6, the transform was taken only on the part of the decay recorded after complete field reversal. The notation of the beats is that detailed in Figure 2.

where $g_F$ is the Landé $g$-factor of the hyperfine state and $\mu_B$ the Bohr magneton, respectively. Throughout this work we define $Z$ as the initial magnetic field direction and apply the diabatic representation, *i.e.* the coordinate system remains fixed in space and does not follow the magnetic field direction. We expand the Hamiltonian as [31]

$$\mathbf{H} = \mathbf{H_0} + g_F \mu_B (B_X F_X + B_Y F_Y + B_Z F_Z). \qquad (2)$$

In the case of a unidirectional field, the Zeeman matrix elements are diagonal in $M_F$, otherwise there are cross-terms requiring numerical integration. The fluorescence intensity is then obtained from $I_F \sim \mathrm{Tr}(\varrho L_F)$, where $L_F$ is the fluorescence monitoring operator.

The time dependence of the switched magnetic field was taken from our previous work [8] with the total field strength following the expression $B(t) = B_\infty$ for $t < t_0$ and $B(t) = B_\infty(1 - 2e^{-(t-t_0)/\tau})$ for $t \geq t_0$. The rise time $\tau$ is $\sim 80$ ns [9]. Initial simulations were performed for the case of linearly polarized excitation without field reversal and the results were compared with Figure 3. The results verified the hyperfine splitting measured previously and found the $g_F$ factors to be well described by the weak field expression

$$g_F = \frac{F(F+1) + J(J+1) - I(I+1)}{2F(F+1)} g_J. \qquad (3)$$

Due to the nature of quantum beat spectroscopy, the sign of $g_J$ cannot be directly obtained but the magnitude was determined as $|g_J| = 0.051$.

As an example, we present in Figure 7 the Fourier transforms of simulations of the decays taking place in a constant magnetic field $B_0$ (dotted trace) and in a field which is reversed after $t_0 = 0.8$ $\mu$s (solid trace). The traces show the same behavior as observed in the experiment (Fig. 6), namely the 0.26 MHz shift of the beat frequency (from 5.52 to 5.78 MHz). We note that for the simulation the reversal of the field does not have any influence on the coherence strength, as the two peaks have an identical height. Furthermore, we studied the influence of weak static magnetic fields with arbitrary direction, but no effect could be discerned for field strengths which are of the order of residual static fields in the experiment.

## 5 Discussion

The results described above demonstrate the preparation, the manipulation of the populations and the detection of specific spin states in the molecule $^{13}CS_2$ illustrated by the level scheme of Figure 2. Coherently excited hf levels in an electronically excited state were subjected to a rapidly switched magnetic field which reversed its field strength from $B$ to $-B$. Before, during and after this process the time evolution of the emission of selected hf levels were monitored by quantum beat spectroscopy. This was achieved by using circularly polarized excitation and the appropriate geometry to prepare only one, representative coherence among the levels $\left|F' = \frac{3}{2}, M'_F = \frac{1}{2}\right\rangle$ and $\left|\frac{1}{2}, \frac{1}{2}\right\rangle$ as depicted in Figure 6. The magnetic field reversal under our experimental conditions is unidimensional (*i.e.* the field changes from $B_Z$ to $-B_Z$). The orientation of the molecular angular momentum in terms of $\mathbf{F} = \mathbf{J}+\mathbf{I}$ cannot follow the field, as this requires the presence of a transverse component yielding off-diagonal matrix elements in $M'_F$. Thus the direction of the molecular magnetic moment after switching has a different (antiparallel) orientation with respect to the external magnetic field than before, reminiscent of a Majorana spin-flip. The energy of the occupied hf levels is therefore changed by the field reversal process. This is best visualized using the diabatic representation (see Sect. 4) in which the energy ordering of the hf Zeeman levels is reversed after field reversal. Accordingly, the energy of the $\left|\frac{3}{2}, \frac{3}{2}\right\rangle$ level is reduced by –0.77 MHz, that for the $\left|\frac{3}{2}, \frac{1}{2}\right\rangle$ level by –0.26 MHz, and that for $\left|\frac{1}{2}, \frac{1}{2}\right\rangle$ by –0.51 MHz when the magnetic field is reversed from 5.4 to –5.4 G. This is manifested by a blue shift of 0.26 MHz in the frequency of the selected coherence in Figure 6 from

quantum beat (c) to (d). In contrast to our previous work [8,9] with linearly polarized excitation, the field reversal leads to a net exchange of energy between the molecule and the magnetic field. The slight reduction ($\sim$10 %) in the magnitude of the quantum beat after switching reveals a small decrease in the strength of the resulting coherence. We attribute this loss to imperfections in the experiment such as spurious magnetic fields. Although our simulations indicate that residual static magnetic fields cannot be responsible for this effect, it is possible that the switching of the electric current may itself induce transverse fields causing this slight loss of coherence.

We emphasize the fact that after switching, no evidence was found for the presence of the initially observed beat, an indication that a negligible amount of population is transferred into the levels $\left|\frac{3}{2},-\frac{1}{2}\right\rangle$ and $\left|\frac{1}{2},-\frac{1}{2}\right\rangle$ as labeled in the diabatic representation. This result of our switched field experiment is clearly different from former works on Majorana transitions which were performed using continuous atomic beams and static magnetic fields [12,13,18,19]. In this case, it is difficult to obtain a Majorana spin-flip for the entire ensemble of particles because of the unavoidable spatial extension of such a particle beam. The atoms which pass at a finite distance from a field reversal point will experience a transverse magnetic field which is a consequence of the relation "div $\mathbf{B} = 0$", and which may induce transitions to other magnetic sublevels with the result that their spin (adiabatically) follows the direction of the magnetic field.

Numerical simulations based on a density matrix method were found to reproduce the experimental results, with the exception that in the simulations the transfer of coherence was found to be 100 % efficient.

## 6 Conclusion

In this work we have applied quantum beat spectroscopy to study the effect of magnetic field reversal on molecular coherences: in this case coherences among hf levels in $^{13}CS_2$. A single coherence was prepared using circularly polarized excitation and the coherence induced after field reversal was analyzed. Using a switched magnetic field as detailed in our previous work, we find the initial coherence among the levels $\left|\frac{3}{2},\frac{1}{2}\right\rangle$ and $\left|\frac{1}{2},\frac{1}{2}\right\rangle$ to be conserved to 90 % if labeling is performed using the diabatic representation. This is equivalent to a Majorana transition and is, to our knowledge, the first such observation in a molecular system. Importantly no coherence was found to be transferred into the coherence $\left|\frac{3}{2},-\frac{1}{2}\right\rangle$ and $\left|\frac{1}{2},-\frac{1}{2}\right\rangle$ indicating the amount of adiabatic transitions to be very small. The 10 % coherence loss is attributed to dephasing caused by stray fields due to the switching process. The use of numerical simulations based on a density matrix method facilitated the analysis process and fully supports our interpretation.

Support of this work by the Schweizerischer Nationalfonds zur Förderung der wissenschaftlichen Forschung is gratefully acknowledged. We thank Prof. Karl Lendi for helpful discussions during this work.

## References

1. S. Haroche, in *High-Resolution Laser Spectroscopy*, edited by K. Shimoda (Springer, Berlin, 1976).
2. E.B. Alexandrov, M.P. Chaika, G.I. Khvostenko, *Interference of Atomic States*, Vol. 7 of *Atoms and Plasmas* (Springer, Berlin, 1993).
3. E. Hack, J.R. Huber, Int. Rev. Phys. Chem. **10**, 287 (1991).
4. H. Bitto, J.R. Huber, in *Nonlinear Spectroscopy for Molecular Structure Determination*, edited by R.W. Field, E. Hirota, J.P. Maier, S. Tsuchiya (Blackwell Science, Oxford, 1998).
5. H. Bitto, J.R. Huber, Opt. Commun. **80**, 184 (1990).
6. H. Bitto, A. Levinger, J.R. Huber, Z. Phys. D **28**, 303 (1993).
7. A. Levinger, H. Bitto, J.R. Huber, Opt. Commun. **103**, 381 (1993).
8. H. Ring, R.T. Carter, J.R. Huber, Eur. Phys. J. D **4**, 73 (1998).
9. H. Ring, R.T. Carter, J.R. Huber, Laser Phys. **9**, 253 (1999).
10. E. Majorana, Nuovo Cimento **9**, 43 (1932).
11. P.Güttinger, Z. Phys. **73**, 169 (1931).
12. T.E. Phipps, O. Stern, Z. Phys. **73**, 185 (1931).
13. R. Frisch, E. Segrè, Z. Phys. **80**, 610 (1933).
14. N.F. Ramsey, *Molecular Beams* (Clarendon Press, Oxford, 1985).
15. F. Bloch, I. Rabi, Rev. Mod. Phys. **17**, 237 (1945).
16. R.T. Robiscoe, Am. J. Phys. **39**, 146 (1971).
17. R.D. Hight, R.T. Robiscoe, W.R. Thorson, Phys. Rev. A **15**, 1079 (1977).
18. R.D. Hight, R.T. Robiscoe, Phys. Rev. A **17**, 561 (1978).
19. W. Schröder, G. Baum, J. Phys. E: Sci. Instrum. **16**, 52 (1983).
20. S. Urabe, Y. Ohta, Y. Saburi, IEEE Trans. Instrum. Meas. **33**, 117 (1984).
21. L. Windholz *et al.*, Phys. Rev. Lett. **77**, 2190 (1996).
22. M.B. Plenio, P.L. Knight, Phys. Rev. A **53**, 2986 (1996).
23. R.G. Unanyan, L.P. Yatsenko, K. Bergmann, B.W. Shore, Opt. Commun. **139**, 48 (1997).
24. B. Kleman, Can. J. Phys. **41**, 2034 (1963).
25. C. Jungen, D.N. Malm, A.J. Merer, Can. J. Phys. **51**, 1471 (1973).
26. D.T. Cramb, H. Bitto, J.R. Huber, J. Chem. Phys. **96**, 8761 (1992).
27. H. Bitto, A. Ružičić, J.R. Huber, Chem. Phys **189**, 713 (1994).
28. J.T. Hougen, J. Chem. Phys. **41**, 363 (1964).
29. K. Blum, *Density Matrix Theory and Applications* (Plenum Press, New York, 1996).
30. A. Corney, *Atomic and Laser Spectroscopy* (Clarendon Press, Oxford, 1977).
31. C.H. Townes, A.L. Schawlow, *Microwave Spectroscopy* (Dover, New York, 1975).